Accepted Manuscript

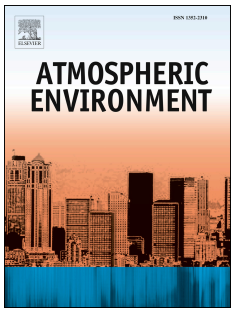

Rainwater capacities for BTEX scavenging from ambient air

A. Šoštarić, S. Stanišić Stojić, G. Vuković, Z. Mijić, A. Stojić, I. Gržetić

PII: S1352-2310(17)30558-7

DOI: 10.1016/j.atmosenv.2017.08.045

Reference: AEA 15515

To appear in: *Atmospheric Environment*

Received Date: 14 March 2017

Revised Date: 15 August 2017

Accepted Date: 18 August 2017

Please cite this article as: Šoštarić, A., Stanišić Stojić, S., Vuković, G., Mijić, Z., Stojić, A., Gržetić, I., Rainwater capacities for BTEX scavenging from ambient air, *Atmospheric Environment* (2017), doi: 10.1016/j.atmosenv.2017.08.045.

Rainwater capacities for BTEX scavenging from ambient air

A. Šoštarić[1*], S. Stanišić Stojić[2], G. Vuković[3], Z. Mijić[3], A. Stojić[3] and I. Gržetić[4]

1 Institute of Public Health Belgrade, Bulevar Despota Stefana 54a, 11000 Belgrade, Serbia

2 Faculty of Physical Chemistry, University of Belgrade, Studentski trg 12-16, 11000 Belgrade, Serbia

3 Institute of Physics Belgrade, University of Belgrade, Pregrevica 118, 11080 Belgrade, Serbia

4 Faculty of Chemistry, University of Belgrade, Studentski trg 12-16, 11000 Belgrade, Serbia

*Corresponding author: andrej.sostaric@zdravlje.org.rs; Phone: +381 64 13 94 185; Fax: +381 11 32 35 080; Bulevar Despota Stefana 54a, 11000 Belgrade, Serbia.

Abstract

The contribution of atmospheric precipitation to volatile organic compound (VOC) removal from the atmosphere remains a matter of scientific debate. The aim of this study was to examine the potential of rainwater for benzene, toluene, ethylbenzene and xylene (BTEX) scavenging from ambient air. To that end, air and rainwater samples were collected simultaneously during several rain events that occurred over two distinct time periods in the summer and autumn of 2015. BTEX concentrations in the gaseous and aqueous phases were determined using proton transfer reaction mass spectrometry. The results reveal that the registered amounts of BTEX in rainwater samples were higher than those predicted by Henry's law. Additional analysis, including physico-chemical characterization and source apportionment, was performed and a possible mechanism underlying the BTEX adsorption to the aqueous phase was considered and discussed herein. Finally, regression multivariate methods (MVA) were successfully applied (with relative errors from 20%) to examine the functional dependency of BTEX enrichment factor on gaseous concentrations, physico-chemical properties of rainwater and meteorological parameters.

Keywords: BTEX, wet deposition, rain, PTR-MS, multivariate methods, Unmix.

1. Introduction

Benzene, toluene, ethylbenzene and the three xylene isomers, frequently referred to as BTEX, constitute a group of aromatic hydrocarbon species of particular environmental interest, commonly associated with the petrochemical industry and incomplete fossil fuel oxidation (Stojić et al. 2015a; Stojić et al., 2015b). Besides being important photochemical precursors for tropospheric ozone and secondary organic aerosols (SOA) (Chatani et al., 2015), these hazardous air pollutants cause chronic toxicity even in small concentrations (Stojić et al., 2015c). According to the IARC data, benzene is recognized as a significant public health threat and classified as group I carcinogen, ethylbenzene is a suspected IIB carcinogen, while both toluene and the xylene isomers belong to group III neurotoxins (WHO, 1986, 1993, 1997; Durmusoglu et al., 2010).

In the atmosphere, volatile species are distributed between the gaseous, aqueous and particle phase (Matsumoto et al., 2010). In their biogeochemical cycle, it is believed that the role of atmospheric water is quite prominent, but this issue is still subject to continuous scientific debate (McNeill et al., 2012). The concentrations of BTEX in various forms of atmospheric water depend on various factors including their ambient gas mixing ratios, water solubility and Henry's law constant, frequency and intensity of precipitation events (Balla et al., 2014), gas-water surface interactions (Raja and Valsaraj, 2004), content and concentrations of other species in atmospheric water (Okochi et al., 2005; Sato et al., 2006; Allou et al., 2011), as well as the origin of air masses (Mullaugh et al., 2015). Previous studies, which primarily focused on wet deposition of BTEX and their partition between gaseous and aqueous phases, were relatively scarce and provided contradictory conclusions.

In the study aimed at investigating the capacity of rainwater for wet scavenging of BTEX, Okochi et al. (2004) reported that the concentrations of species detected in rain samples were higher than those predicted by Henry's law, and concluded that atmospheric precipitation might play significantly greater role in removing BTEX from ambient air than previously thought. Thereby, the observed supersaturation was assumed to be associated with the presence of surface-active agents in rain droplets, whereas the rainfall intensity appeared to be of negligible importance. Accordingly, our previous study confirmed a significant enrichment of BTEX in the aqueous phase in a dynamic equilibrium system designed to resemble the interactions between the gaseous and water phase during rainfall (Šoštarić et al., 2016). Conversely, recent findings of Mullaugh et al. (2015) indicate that BTEX were not efficiently scavenged from the atmosphere by wet deposition processes. Furthermore, the authors concluded that light-mediated reactions with OH· or nitrogen radicals remain the major atmospheric sink for BTEX. Nonetheless, it should be noted that this research was

not based on the ambient air measurements, but it mainly relied on the previously published BTEX data from similar locations.

In order to better understand the fate of volatile species in atmospheric, terrestrial and aquatic systems, the present study examines the contribution of rainwater to wet scavenging of atmospheric BTEX, as well as the mechanisms related to their air-water distribution transfer.

2. Materials and methods

A total of 53 sample pairs of air and rainwater samples were collected simultaneously during several rain events that occurred over two distinct time periods in the summer and autumn season of 2015. The sampling was performed at the Institute of Physics (Belgrade, Serbia; 44°49' N, 20°28' E), located in the vicinity of the Danube river, in the suburban residential area, with a number of local fireboxes active during the heating season.

Rainwater sampling was performed using a custom-built precipitation collector with the effective sampling area of 9 m^2. The steep collecting panels (45°) were designed to reduce rainfall retention time and minimize possible BTEX volatilization. Such large sampling area enabled collecting a vast number of samples per each rain event. The panels were thoroughly rinsed with 18 MΩ ultrapure water (ELGA PURELAB maxima system) prior to each sampling campaign, and the rinsing water was collected and analyzed as a field blank control sample. No target compounds were detected in the field blank control samples. The samples were collected and stored directly into brown glass bottles of 1300 mL. All bottles were washed with detergent, thoroughly rinsed with ultrapure water and dried in an oven for two hours at 105°C to remove any trace of contamination. During the sampling, the bottles were filled to the top to avoid headspace, and the sampling duration and sample temperature were recorded. Since sampling equipment enables collection of large volumes of rainwater within a short period, the last sample in each sampling campaign was collected in the bottle of 2,600 mL and was split into two standard aliquots. The first aliquot was analyzed immediately, whereas the other one was examined after all other samples to determine whether the BTEX levels changed over time. No difference could be observed in the obtained quantity of double samples (Table S1, Supplementary material).

BTEX concentrations in both gas and water phases were measured using proton transfer reaction mass spectrometer (Standard PTR-quad-MS, Ionicon Analytik, GmbH, Austria), whose detailed description is given elsewhere (Lindinger et al., 1998). Since PTR-quad-MS is not capable of distinguishing isobaric ions, the signal detected at m/z 107 referred to C_8 aromatic hydrocarbons, ethylbenzene, o-, m-, and p-xylene. Signals detected at m/z 79 and m/z 93 referred to benzene and toluene, respectively (Warneke et al., 2003).

The air samples were collected as a side flow from a 1/8-inch teflon tube sampling line through which ambient air was drawn at the flow rate of about 50 L min^{-1} to ensure short residence. The sample inlet was located 6 m above ground level with a sampling angle of 360°. Drift tube parameters included: pressure, ranging from 2.04 to 2.14 mbar; temperature, 60 ^{0}C; voltage, 600 V; E/N parameter, 145 Td providing reaction time of 90 µs. The count rate of $H_3O^+H_2O$ was 3 to 8% of the $9.2 \cdot 10^6$ counts s^{-1} count rate of primary H_3O^+ ions. PTR-MS calibration was performed before and after each sampling campaign using an external standard five-point calibration, ranging from 0-26 ppbV, 0-25 ppbV and 0-80 ppbV for B, T and EX, respectively. For this purpose, 2.5 ppmV mixture of BTEX (BTEX in nitrogen, Messer Group GmbH) was diluted with high-purity synthetic air (CH free, Messer Group GmbH) by means of HORIBA ASGU 370-P system.

Determination of BTEX concentrations in rainwater was performed immediately after each sampling campaign. A liter of each unfiltered rainwater sample was transferred to the gas washing bottle (GWB) and purged out with synthetic air at a flow rate of 1 L min^{-1}. Rainwater filtration was avoided due to potential adsorption of species on the filter. The GWB output was connected with PTR-MS

inlet via T-piece, and further analytical procedure, calibration and data processing were conducted as described in Šoštarić et al. (2016). In brief, PTR-MS signal obtained during exsufflation was subject to baseline fitting. The exsufflation time was determined for each sample as the interval required for equilibrium to be achieved (t_{eq}). The obtained exsufflation time was used for determining the amounts of target compounds retained in the analyzed rainwater samples. The aqueous concentrations of analyzed species were calculated by multiplying the obtained amounts by the conversion factor (3.25; 3.83 and 4.41 for B, T and EX, respectively). The detection limits (DL) in rainwater were determined using HC free air and calculated as 10 nM, 10 nM and 20 nM for B, T and EX, respectively. The remaining portion of each rainwater sample was transferred to a 300-mL bottle and stored at 4°C until further analysis, which included determination of the major inorganic anions (F^-, Cl^-, SO_4^{2-}, NO_2^- and NO_3^-), dissolved cations (Na^+, NH_4^+, K^+, Ca^{2+} and Mg^{2+}), total organic carbon, electrical conductivity, UV extinction, turbidity and pH, in accordance with the standard methods (US EPA 300.1:1993, EN ISO 14911:1998, ISO 8245:1999, EN 27888:1993, SMEWW 19th method 5910 B, US EPA 180.1:1993, EN ISO 10523:2008, respectively). More details of the methods and equipment applied for physico-chemical analysis conducted on rainwater samples are presented in Supplementary material.

In order to determine the extent to which Henry's law constant (K_H) describes BTEX distribution between the gaseous and aqueous phase, distribution coefficients (D_{OBS}) were calculated for each sample pair and each species, as the ratio of the corresponding experimentally derived rainwater concentrations in nM (C_R) and ambient gas phase mixing ratios in ppbV (p_g):

$$D_{OBS} = {}^{C_R}/_{p_g} \ (M\ atm^{-1}) \quad (1)$$

Furthermore, the enrichment factors (EF) were calculated as the ratio of D_{OBS} and K_H.

Considering the K_H temperature dependence, EF were calculated using temperature corrected K_HT for each rain sample by means of the following equation (Sander, 2015):

$$K_HT = K_H(298.15)exp\left\{\frac{-\Delta H}{R}\left(\frac{1}{298.15} - \frac{1}{T}\right)\right\} \quad (2)$$

where K_H is the Henry's law constant at 298.15 K for pure water, ΔH is the enthalpy change of air-water transfer, T is the rainwater temperature, and R is the universal gas constant (8.314 J K^{-1} mol^{-1}). Furthermore, to assess the representativeness of ground level conditions for the atmospheric conditions during rainfall, K_HT and EF altitude profiles were calculated using the temperature profiles obtained from GDAS1 (Global Data Assimilation System, 2015), by replacing the rainwater temperature value by the temperature at the corresponding altitude.

Meteorological parameters during rain events (precipitation (accumulated rainfall, rain current and peak intensity, and the duration of a rain event), wind speed and direction, pressure, humidity and temperature) were measured by Vaisala Weather Transmitter WXT530 Series. Cloud information, including cloud height and type, was obtained from the airport "Nikola Tesla", Belgrade, ICAO code LYBE, located 8.9 km SSW from the sampling site.

The relationships between enrichment factors (EF), physico-chemical characteristics and wind characteristics (wind speed and direction) were examined using the bivariate polar plot analyses (Carslaw and Beevers, 2013) implemented in the Openair package (Carslaw and Ropkins, 2012) within the statistical software environment R (Team, 2012).

The neutralization factors (NF) were calculated based on the study of Moreda-Piñeiro et al. (2014), Tiwari et al. (2016) and references therein in order to examine the potential of the cations to balance the rainwater acidic components:

$$[NF_{Ca^{2+}}] = \frac{[nss\mathrm{Ca}^{2+}]}{NO_3^- + [nss\mathrm{SO}_4^{2-}]} \quad (3)$$

$$\left[NF_{Mg^{2+}}\right] = \frac{[nss\mathrm{Mg}^{2+}]}{NO_3^- + [nss\mathrm{SO}_4^{2-}]} \quad (4)$$

$$\left[NF_{NH_4^+}\right] = \frac{[\mathrm{NH}_4^+]}{NO_3^- + [nss\mathrm{SO}_4^{2-}]} \quad (5)$$

$$[NF_{K^+}] = \frac{[nss\mathrm{K}^+]}{NO_3^- + [nss\mathrm{SO}_4^{2-}]} \quad (6)$$

To calculate the non-sea salt fraction of any particular ion (*nss*), we assumed that all Na originated from marine sources, and used it as a referent element. The nss contribution is given as:

$$[nss - X]_i = [X_i] - [Na^+]_i \left[\frac{[X]}{Na^+}\right]_{sea\ salt} \quad (7)$$

where [nss - X]$_i$ is the nss concentration of the selected ion in the sample *i*, [X$_i$] is the total concentration of the ion X measured in the rainwater sample *i*, [Na^+] is the total concentration of Na^+ measured in the rainwater sample, and $[[X][Na^+]^{-1}]_{seasalt}$ is the reference ratio determined in the seawater.

Potential remote source regions that might affect the observed BTEX mixing ratios were identified using HYSPLIT-derived 72-h back trajectories (Draxler and Rolph, 2014). The trajectories were computed for each hour UTC a day before and during each rain event, above the sampling location at the half of the planetary boundary layer height calculated from GDAS1 using MeteoInfo (Wang, 2014), as described in Stojić at al. (2016) and Stojić and Stanišić Stojić (2017).

Rainwater source apportionment was performed using Unmix (USEPA, 2007). The maximum number of species selected as input variables was chosen using the trial and error with the overall aim of yielding the most physically meaningful results. For concentrations below the DL, a value equal to the half of the DL was used.

Guided regularized random forest (GRRF) was applied (Deng and Runger, 2013) for the selection of features that are most relevant for EF. Random forest (RF) consists of a number of decision trees which every node represents a condition on a single variable designed to split the dataset in two parts so that similar response values end up in the same set. Variable importance measures how much each variable decreases the weighted impurity across all tress, a measure based on which the optimal condition is chosen. GRFF uses the importance scores from a preliminary RF to guide the feature selection of regularized random forest (RRF), and has several advantages as follows: it is more robust and computationally efficient than RRF, varSelRF and LASSO logistic regression; it can select compact feature subsets moderating the curse of dimensionality; it avoids the effort to analyze irrelevant or redundant features; and it has competitive accuracy performance. Variable importance presented herein was obtained by calculating the average value of 2000 GRRF runs. The appropriate number of trees was determined to assure out-of-bag error convergence. Method performance was tested by 100 times replicated 10-fold cross validation.

To analyze the relationship between EF and features that are considered most relevant for EF prediction, the following 24 regression MVA methods implemented in Weka 3.8 (Hall et al., 2009) were applied: Alternating Model Tree, Conjunctive Rule, Decision Stump, Decision Table, Elastic Net, Gaussian Processes, IBk, IBkLG, Isotonic Regression, K*, Least Median Squared, Linear Regression, Locally Weighted Learning, M5P, M5 Rules, Multilayer Perceptron, Pace Regression, Random Forest, Random Tree, Radial Base Function (RBF) Network, RBF Regressor, REP Tree, Simple Linear Regression and SMOreg Support Vector Machine. A brief description of the methods, including functions (neural network, support vector machine, etc.), clustering techniques, rules and trees, is provided in Supplementary material. Method performance was tested by 10 times replicated 10-fold cross-validation.

3. Results and discussion

Light showers, with occasional thunderstorms, constituted a considerable part of summer rain events. Scattered and broken clouds in the form of cumulonimbus or towering cumulus were observed at the height of 400 to 1000 m. In the autumn campaign, the vast majority of rain events were light and sporadically followed by mist. Scattered clouds were registered at levels below 300 m, whereas broken clouds were observed from 100 to 900 m.

As expected, both aqueous and gaseous BTEX concentrations were higher during the cold part of the year. Lower BTEX concentrations in summer can be attributed to intense photochemical removal and washout effects associated with more sunny and rainy days (Lee et al., 2002), whereas higher concentrations of BTEX in autumn can be associated with individual combustion fireboxes widely spread in the vicinity of the sampling site. Furthermore, aqueous B concentrations in summer were below DL.

As can be seen in Figure 1, each rain event was associated with air masses coming from different source regions and heights. During summer rain events, air flows from all directions were followed by significant variations in physico-chemical properties of rainwater, whereas N and NE air masses in autumn were associated with a more uniform rainwater composition. Gaseous concentrations of volatile species, particularly B, were relatively stable during rain events, which can be explained by the fact that the sampling site was dominated by local BTEX sources.

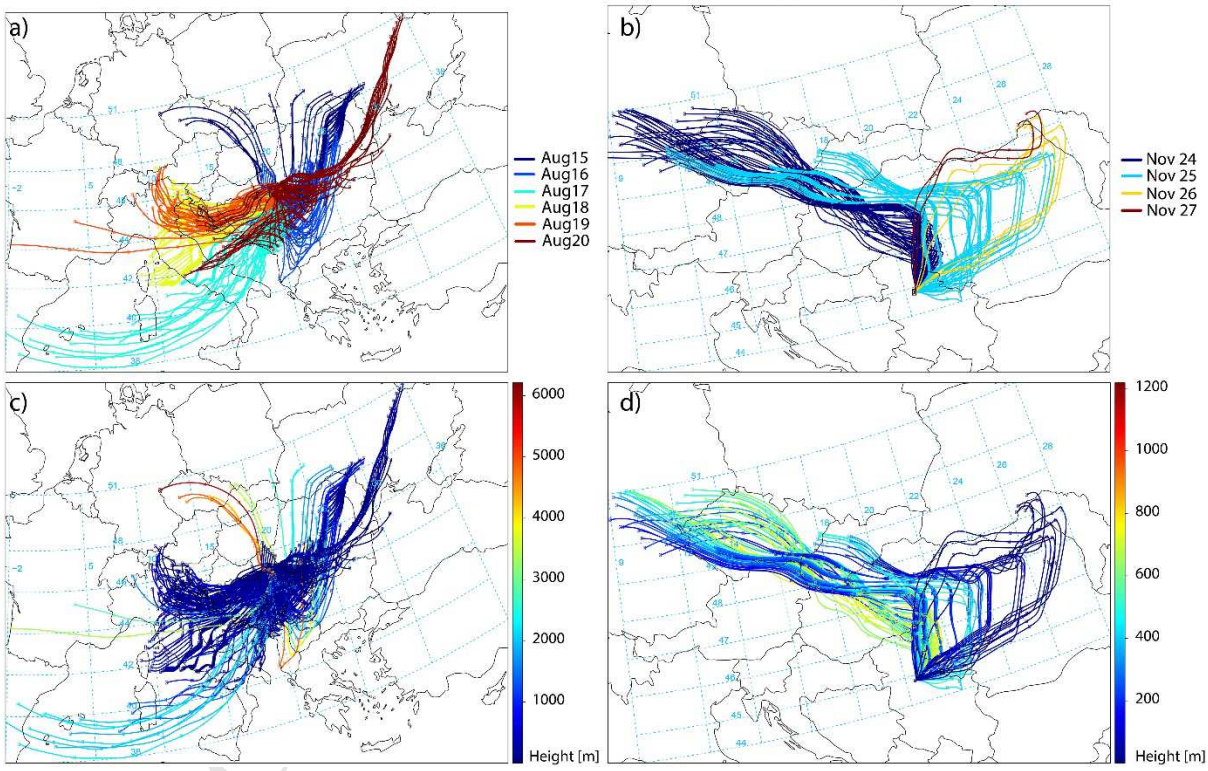

Figure 1. Back trajectories a day before (August 15 and November 24) and during summer (a) and autumn (b) rain events and corresponding trajectory heights (c, d).

3.1 Physico-chemical characteristics of rainwater

Basic statistics for all rainwater parameters and BTEX concentrations is given in Table S2, Supplementary material. The average rainwater pH was 6.01, while the turbidity was below 10 NTU, indicating that the samples contained moderate amounts of suspended particles from the atmosphere. As illustrated in Figure S1, conductivity, as well as high concentrations of most ions (SO_4^{2-}, NO_3^-, Ca^{2+}, Mg^{2+}, K^+ and Na^+) were influenced by the high-speed SW wind (20 to 30 m s^{-1}), while only NH_4^+ concentrations were increased with the wind of moderate speed (10 m s^{-1}) from NE direction.

The rainwater pH varied from 3.70 to 8.20 with the volume weighted mean of 6.01, which is mainly due to scavenging of alkaline species (Ca^{2+} and SO_4^{2-}). The average pH value is also close to the 5-year-mean (6.1) obtained as a part of the regular air quality monitoring in Belgrade. The contribution of SO_4^{2-} to the rainwater acidity was confirmed by ($Cl^- + NO_3^-$) and (SO_4^{2-}) ratio below 1 (Tiwari et al., 2016). As shown, Ca^{2+} was the dominant neutralization component, followed by NH_4^+, Mg^{2+} and K^+, with mean of 77%, 14%, 7% and 2.3%, respectively.

As shown in Figure S2, significant correlations were observed as follows: > 0.80 (NO_3^- – SO_4^{2-}, NH_4^+ – aq. B, NH_4^+ – gas. B, NH_4^+ – EF_B); 0.70 – 0.80 (F^- – SO_4^{2-}, F^- – NO_3^-, F^- – aq. B, F^- – gas. B, F^- – EF_B, K^+ – Na^+); and 0.60 – 0.70 (NO_3^- – Mg^{2+}, SO_4^{2-} – Mg^{2+}, SO_4^{2-} – EF_{EX}, Na^+ – Mg^{2+}). Furthermore, high correlations were noted between aq. and gas. BTEX concentrations (≥ 0.80), as well as between aq. EX and aq. B (0.67) and aq. T (0.67), suggesting that these species might share the common source.

As can be seen in Tables S3, S4 and S5, four factors were derived using Unmix. With high contributions of volatile BTEX species (99%, 44.5% and 52.2%) and a relatively high share of UV extinction (33.3%), the first factor was recognized as organic compounds in the gaseous form. The second factor, characterized by the highest contribution of TOC (71.6%) and turbidity (79.7%), represented the solid fraction dissolved in the atmospheric water. Significant shares of K^+ (58.0%), SO_4^{2-} (42.2%) and NO_3^- (31.3%) were also apportioned to this factor, as a result of fossil fuel burning and traffic exhaust (Rao et al., 2016; Tiwari et al., 2016). The high shares of crustal-related elements, Na^+ (61.8%) and Mg^{2+} (61.4%), were apportioned to the third factor (Cao et al., 2008; Sapek, 2014). Moderate to significant shares (> 30%) of all species except Na^+, K^+ and B were apportioned to the fourth factor, being recognized as the aerosol fraction. Apart from gaseous oxides (SO_2 and NO_2), which react with ozone and OH· radicals in the presence of Ca^{2+} and Mg^{2+} (Seinfeld and Pandis, 2006), BTEX are susceptible to photo-oxidation that can also lead to SOA formation. BTEX reactions include oxidation with ozone and OH·, but also with NO_x and SO_2, which results in multi-functional oxy products that are further deposited onto the existing aerosol or initiate the formation of SOA by self-nucleation. BTEX behave differently in the atmosphere due to differences in the methyl chain substituent and the alkyl chain length. Benzene is considered being extremely stable compared to T and EX (Słomińska et al., 2014), and it is less susceptible to the heterogeneous reactions and formation of SOA in the atmosphere.

The contributions of the gaseous organic- and aerosol-related factors were mostly associated with N wind of moderate speed (< 10 m s^{-1}), which clearly reflects their local origin, while the solid- and crustal-related factors were associated with the air masses from SW direction and high wind speed (20 to 30 m s^{-1}) (Figure S3). The contribution of the factor assigned to aerosols declined during rain events due to wet deposition, while similar behavior was not observed for other factors.

TEX air mixing ratios and rain concentrations decreased during the first two hours of the rainfall, but tend to rise afterwards probably as a result of rainfall intensity decrease (Figure S4, Supplementary material). The highest TEX enrichment, caused by air mixing ratio decrease, was detected during the second hour. Typical washout effect was observed for source contributions related to the rainwater aerosol and solid components, and was less pronounced for crustal factor. Unlike TEX, only a slight decrease in benzene air mixing ratios was noticeable, which is reflected in a constant EF_B increase.

3.2 BTEX distribution between gaseous and aqueous phases

The exsufflation time required for the equilibrium to be achieved was different for rainwater samples and ultrapure water, which suggests that physico-chemical properties and BTEX content distributed between different phases have certain impact on the adsorption to the aqueous phase (Figure 2, left). However, the correlations were registered only between the concentrations of B, and F^- (-0.72) and NH_4^+ (0.83) (Figure S2, Supplementary material). The impact of rainwater physico-chemical properties on the BTEX retention was further examined by insufflating 2 ppbV of BTEX in 10 pre-exsufflated rainwater samples, as described in our previous paper (Šoštarić et al., 2015). The results showed slightly longer exsufflation periods for rainwater samples compared to the pure water,

indicating that physico-chemical properties are not the main contributor to the extended retention in the rainwater. The comparative qualitative analysis of rainwater and ultrapure water exsufflation time series obtained by real-time PTR-MS measurements showed that different capacities for BTEX retention can be mainly associated with BTEX aerosol fraction (Figure 2, right).

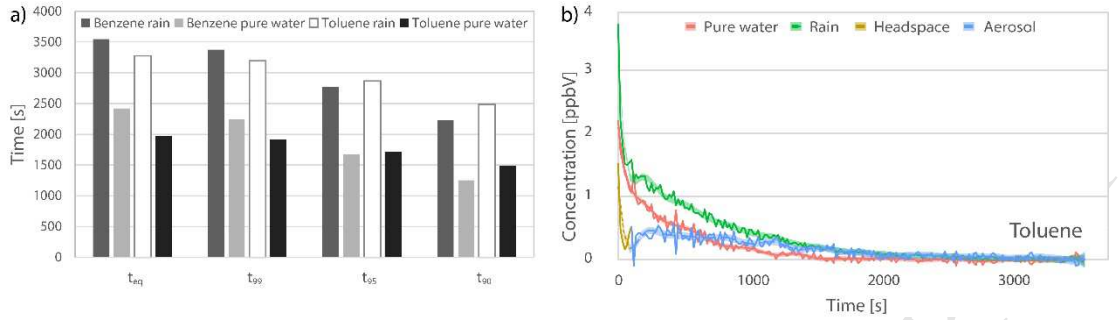

Figure 2. The time required to reach equilibrium (t_{eq}) and 99, 95 and 90% quantity of benzene and toluene to be exsufflated (left), and toluene exsufflation from ultra-pure water and rainwater (right).

Generally, due to very small K_H values of aromatic compounds, BTEX concentrations in rainwater are expected to be low (Słomińska et al., 2014). However, according to the results, EF values were in the range from 61 to 128, from 8 to 209, and from 25 to 295 for B, T and EX, respectively, indicating that the BTEX amounts in the aqueous phase significantly exceeded the theoretically predicted levels. Both lower and higher EF values have been reported in the literature. According to the studies dealing with the distribution of chlorinated hydrocarbons and monocyclic aromatic hydrocarbons between air and rainwater, EF ranged from 2.4 to 34 for BTEX (Okochi et al., 2004; Sato et al., 2006), whereas the study of Valsaraj et al. (1993) reported several hundred to a thousand-fold enrichment of hydrophobic organic compounds in fog samples. The enhanced BTEX transfer to urban dew water was also shown by Okochi et al. (2005), with the reported EF values ranging from 7.87 to 20.2. Furthermore, Fries et al. (2007) showed that the concentrations of aromatic hydrocarbons including ethylbenzene, xylenes and 1,2,4-trimethylbenzene, have been significantly lower in rain (15–53 ng L^{-1}) than in snow (71-2200 ng L^{-1}). In the later study, Fries et al. (2008) found that in-cloud scavenging could be a possible explanation for the occurrence of VOC in fallen snow.

Figure 3 illustrates the K_H and EF altitude distribution for BTEX. It should be mentioned that K_H and EF for B and EX exhibit the similar pattern. As can be seen, K_H and consequently EF, change as the raindrop falls to the ground. K_H values calculated using the average temperature on the path of the raindrop differ ±20% from those obtained using the rainwater temperature. Such agreement indicates that the rainwater temperature measured at the ground level is a good indicator of atmospheric conditions under which reactions with BTEX takes place. Moreover, in the study of Lin et al. (2011), it was concluded that, at higher altitudes in locations with dominant local sources, VOC concentrations were generally lower, and hence, higher K_H values would not be expected to affect C_R, nor calculated values of D_{OBS} and EF.

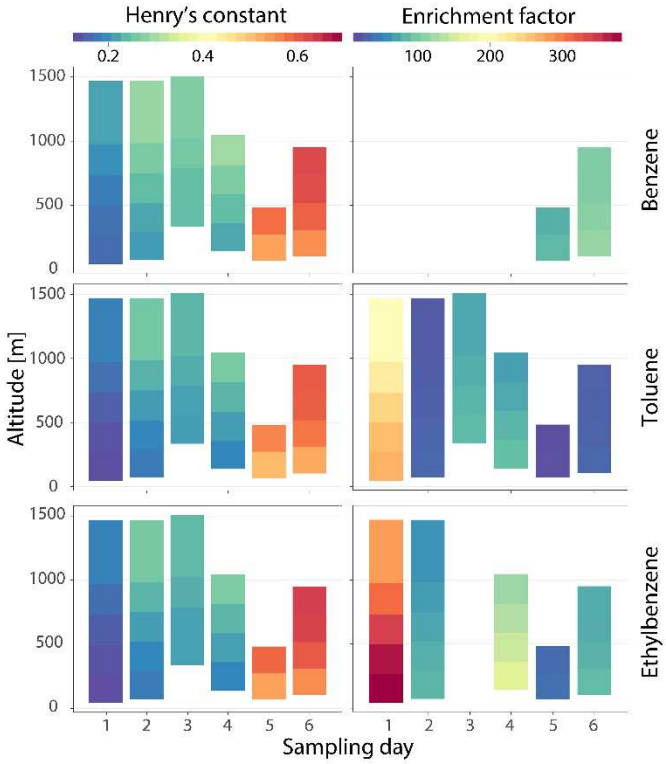

Figure 3. Henry's constant and EF BTEX altitude distributions.

As suggested by the field studies (Valsaraj et al., 1993; Goss, 1994; Okochi et al., 2004; Starokozhev et al., 2009), as well as the laboratory experiments (Bruant and Conklin, 2000; Bruant and Conklin, 2002; Raja et al., 2002; Raja and Valsaraj, 2004; Šoštarić et al., 2016), the interfacial adsorption might be the major mechanism associated with the enhanced VOC transfer to the aqueous phase.

Some previous studies have examined the composition of atmospheric water and the impact of different species, including nitric acid, anionic and nonionic surfactants, as well as the impact of salinity and pH on air-water VOC distribution (O'Sullivan et al., 1996; Vane and Giroux, 2000; Sato et al., 2006; Allou et al., 2011). The supersaturation of VOC in rain samples was explained by decreased rainwater polarity associated with the presence of different organic compounds (Sato et al., 2006). The presence of colloidal organic matter with its large binding capacity for many hydrophobic species was found in fog droplets (Valsaraj et al., 1993). Similarly, in the study of Okochi et al. (2005), the enhanced dissolution of VOC species in urban dew compared to rainwater was explained by the fact that dew forms near the ground and contain more humic-like substances that could lead to a decrease in water surface tension and consequently result in higher VOC enrichment.

The present study considers several factors that could contribute to BTEX enrichment in rainwater, including BTEX concentrations, rainwater physico-chemical properties, rainfall intensity, air masses origin, meteorological conditions and adsorption at the air/water interface.

As regards the physico-chemical characteristics of rainwater, only F^- and SO_4^{2-} can be considered important for the prediction of EF_B (-0.73) and EF_{EX} (0.62), respectively. The latter indicates that SO_2-rich coal burning emissions are also a significant source of EX, while the results for B should be taken with caution due to the small data size.

Higher rainwater T enrichment was mostly observed for low gaseous T concentrations, high TOC (8-12 mg L^{-1}) and turbidity (Supplementary file 1), although the strict link between rainwater enrichment and gaseous concentrations cannot be established. The exsufflation dynamics (Figure 2) and the EF values suggest that prolonged BTEX retention could also be attributed to the adsorption to aerosol fraction. We have considered T partitioning, not only because T concentrations were in a relatively broad range, but also because of the significant number of samples collected in both

seasons with comparable concentrations, despite the fact that similar findings were observed for the rainwater enrichment with EX (Supplementary file 2). As can be observed in Figure 4 and Table S6 of the Supplementary material, higher T enrichment was mostly associated with a higher wind speed at the sampling site (up to 30 m s^{-1}) and air masses coming from SW area, whereas the lowest rainwater enrichment was registered under relatively stable atmospheric conditions (ws < 5 m s^{-1}). Similar associations were also observed for EX. Higher rainwater enrichment could be the result of the prolonged contact time between the aqueous and the gaseous phases, when strong wind-driven raindrops were falling obliquely.

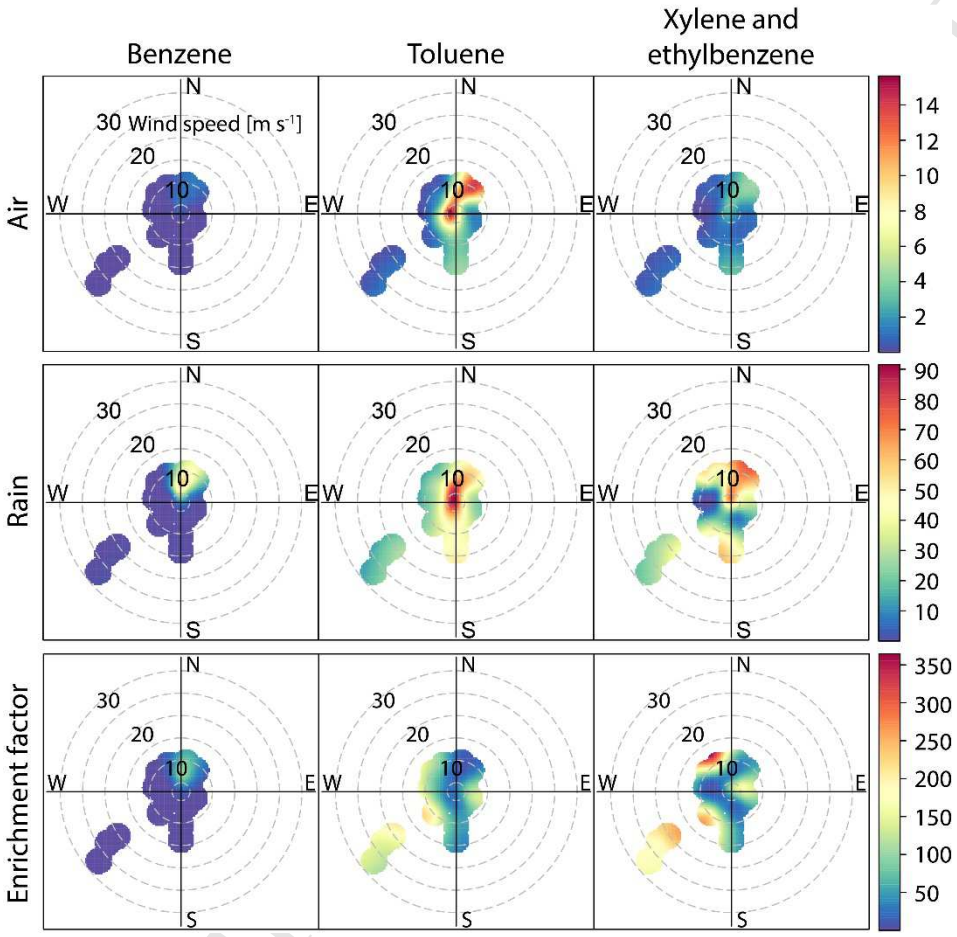

Figure 4. The relationship between BTEX air mixing ratios (ppb), rain concentrations (nM) and enrichment factor and wind characteristics.

According to GRRF results (Table S7, Supplementary material), physico-chemical rainwater properties and gaseous T concentrations appear to be of greater importance than meteorological factors for predicting T and EX rainwater enrichment. Furthermore, these findings also indicate that ground level gaseous concentrations have higher impact on the transfer of species to the aqueous phase than the polluted air masses coming from greater atmospheric heights.

Out of 24 examined MVA regression methods, some of which were previously successfully applied for prediction of PM_{10} and VOC emissions (Stojić et al., 2015d; Perišić, 2016), it has been shown that RF, IBk and IBkLG can provide predictions of EF_T and EF_{EX} based on the variables of the highest importance derived by GRRF with relative errors of approx. 20%, *i.e.* 27%, and correlation coefficients around 0.95 and 0.87, respectively (Table 1). Conversely, the prediction of EF_T and EF_{EX} based on Unmix derived source contributions was less accurate (K*: 36.3% relative error and correlation coefficient 0.79). As can be concluded, functional description of EF_T and EF_{EX} can be based on certain rainwater properties and gaseous T concentrations. In addition to ambient and rainwater B

concentrations, EF_B is affected by meteorological conditions (sample and ambient temperature and Rh), but these results should be taken with caution due to the small B data size.

Table 1. MVA method performance comparison for enrichment factor prediction based on the measured parameters and Unmix-derived source contributions: absolute error, relative error and correlation coefficient (r).

Method	EF_T						EF_{EX}					
	Measured			Unmix derived			Measured			Unmix derived		
	Abs.	Rel.	r	Abs.	Rel.	r	Abs.	Rel.	r	Abs.	Rel.	r
Alternating Model Tree	18.5	34.8	0.88	40.8	76.4	0.67	33.8	42.0	0.78	59.2	111.0	0.53
Conjunctive Rule	26.1	48.9	0.64	32.0	59.9	0.40	39.2	48.7	0.55	43.4	81.2	0.41
Decision Stump	25.5	47.8	0.57	29.3	54.9	0.46	36.4	45.2	0.57	39.4	73.8	0.45
Decision Table	17.8	33.3	0.85	25.3	47.4	0.68	33.9	42.1	0.71	44.8	83.9	0.46
Elastic Net	15.2	28.5	0.88	22.3	41.9	0.77	29.4	36.5	0.74	38.6	72.4	0.62
Gaussian	16.1	30.2	0.88	21.9	41.0	0.79	30.6	38.0	0.72	41.0	76.8	0.60
IBk	11.6	21.7	0.95	20.6	38.5	0.79	22.4	27.8	0.89	31.9	59.8	0.68
IBkLG	11.6	21.7	0.95	20.6	38.5	0.79	22.4	27.8	0.89	31.9	59.8	0.68
Isotonic	13.7	25.7	0.93	31.4	58.9	0.54	34.9	43.3	0.62	39.5	74.0	0.58
K*	11.9	22.3	0.92	19.4	36.3	0.79	22.0	27.4	0.87	31.0	58.1	0.68
Least MedSq	17.4	32.7	0.87	35.6	66.8	0.67	52.7	65.4	0.29	47.4	88.8	0.50
Linear Regression	15.5	29.1	0.89	22.7	42.5	0.78	30.8	38.2	0.74	39.0	73.2	0.61
LWL	15.9	29.7	0.91	26.7	50.0	0.72	35.5	44.1	0.70	39.4	73.9	0.53
M5P	13.9	26.1	0.91	21.6	40.5	0.78	29.7	36.9	0.74	40.4	75.7	0.60
M5Rules	15.0	28.1	0.90	22.9	42.9	0.74	30.8	38.3	0.74	42.2	79.1	0.59
Multilayer	17.7	33.1	0.92	24.2	45.4	0.80	37.5	46.5	0.74	49.5	92.7	0.55
Pace Regression	15.9	29.8	0.88	22.7	42.6	0.77	30.1	37.4	0.74	38.6	72.4	0.62
Random Forest	11.6	21.7	0.95	22.5	42.2	0.76	27.8	34.5	0.76	34.9	65.4	0.62
Random Tree	13.8	25.9	0.89	28.6	53.7	0.59	32.8	40.8	0.67	41.7	78.1	0.54
RBF Network	29.9	56.0	0.45	30.4	57.0	0.65	44.8	55.7	0.49	52.8	98.9	0.40
RBF Regressor	14.7	27.6	0.91	23.6	44.2	0.78	28.1	34.9	0.83	40.9	76.6	0.56
REP Tree	13.9	26.1	0.91	22.5	42.1	0.72	36.9	45.8	0.58	42.0	78.8	0.43
Simple Linear Regression	29.9	56.1	0.49	30.3	56.7	0.55	34.3	42.7	0.71	40.5	75.8	0.61
SMOreg	14.7	27.5	0.88	21.5	40.3	0.79	28.8	35.8	0.75	39.0	73.2	0.61

Figure 5 represents EF for T and EX as a function of their ambient gas phase mixing ratios. As can be seen, EF values increased in summer, due to ambient air temperature, which is one of the most important factors for the decrease of the surface tension leading to enhanced interfacial adsorption (Bruant and Conklin 2000, 2002). Another important feature of Figure 5 is the power functional dependence of EF on ambient gas phase mixing ratios, as adsorption processes are generally more efficient for lower adsorbate concentrations and are characterized by the power functions. These findings are in compliance with the findings of Sato et al. (2006) who showed that rainwater enrichment is especially significant for the species with lower atmospheric concentrations.

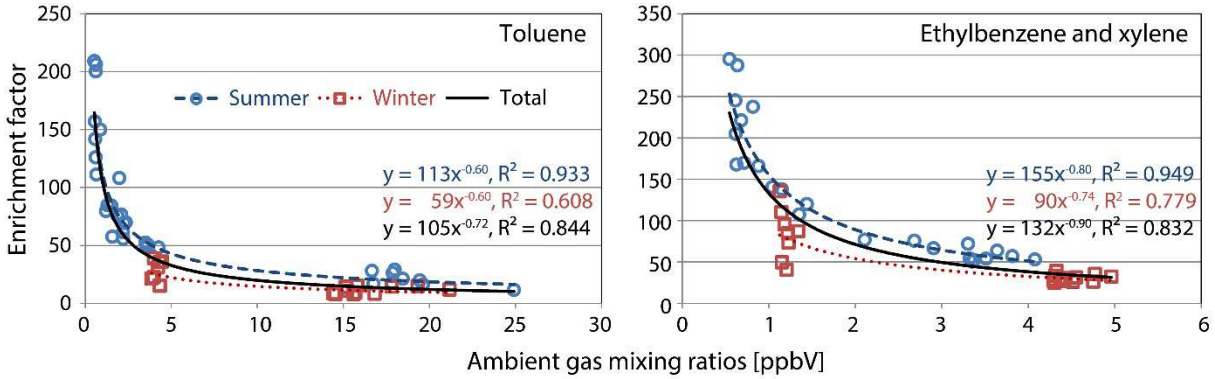

Figure 5. The relationship between T and EX enrichment factors and their gaseous concentrations.

4. Conclusions

The transfer of BTEX and other VOC from the atmosphere to various forms of atmospheric water is an important process that affects the global transport of air pollutants, environmental fate and enables the transfer of these species to terrestrial and aquatic systems. The purpose of this study was to investigate the scavenging potential of rainwater and consider the potential mechanisms and factors associated with this phenomenon.

As shown, BTEX concentrations observed in the aqueous phase exceeded the theoretically predicted values. Given that the interfacial adsorption is assumed to be the major mechanism underlying the enhanced rain scavenging of BTEX, the removal process was observed to be more efficient for lower gas mixing ratios, mainly due to equal surface available for smaller number of molecules and the prolonged contact time between the two phases when wind-driven rain drops were falling obliquely. Accordingly, theoretical predictions are probably more accurate in the area of larger gaseous concentrations, whereas in the case of lower concentrations, transfer to the aqueous phase is often underestimated. Furthermore, the results of the presented regression multivariate analysis suggest that multiple factors determine the spatio-temporal BTEX distribution in the environmental multiphase system, including ambient mixing ratios, physico-chemical properties of rainwater and meteorological data. More specifically, the functional description of EF_T and EF_{EX} can be based on certain rainwater properties. On the other hand, it has been shown that EF_B is affected by meteorological conditions (sample and ambient temperature, and Rh), as well as B ambient and rainwater concentrations (however, these results should be interpreted with caution due to the small B data size).

Acknowledgments

This paper was realized as part of projects No III43007 and No III41011, which were financed by the Ministry of Education, Science and Technological Development of the Republic of Serbia for the period 2011-17, and was supported by the Institute of Public Health of Belgrade, Serbia.

References

Allou, L., El Maimouni, L., Le Calve, S., 2011. Henry's law constant measurements for formaldehyde and benzaldehyde as a function of temperature and water composition. Atmos. Environ. 45, 2991-2998.

Balla, D., Papageorgiou, A., Voutsa, D., 2014. Carbonyl compounds and dissolved organic carbon in rainwater of an urban atmosphere. Environ. Sci. Pollut. Res. 21, 12062-12073.

Bruant, R.G.Jr., Conklin, M.H., 2002. Adsorption of benzene and methyl-substituted benzenes at the vapor/water interface. 3. finite binary-component VHOC adsorption. J. Phys. Chem. B, 106, 2232-2239.

Bruant, R.G.Jr., Conklin, M.H., 2000. Dynamic determination of vapor/water interface adsorption for volatile hydrophobic organic compounds (VHOCs) using axisymmetric drop shape analysis: procedure and analysis of benzene adsorption. J. Phys. Chem. B, 104, 11146-11152.

Cao, J.J., Chow, J.C., Watson, J.G., Wu, F., Han, Y.M., Jin, Z.D., An, Z.S., 2008. Size-differentiated source profiles for fugitive dust in the Chinese Loess Plateau. Atmos. Environ. 42, 2261-2275.

Carslaw, D.C., Beevers, S.D., 2013. Characterising and understanding emission sources using bivariate polar plots and k-means clustering. Environ. Model. Softw. 40, 325-329.

Carslaw, D.C., Ropkins, K., 2012. Openair - An R package for air quality data analysis. Environ. Model. Softw. 27, 52-61.

Chatani, S., Matsunaga, S.N., Nakatsuka, S., 2015. Estimate of biogenic VOC emissions in Japan and their effects on photochemical formation of ambient ozone and secondary organic aerosol. Atmos. Environ. 120, 38-50.

Deng H., Runger G., 2013. Gene selection with guided regularized random forest. Pattern Recognit. 46, 3483-3489.

Draxler, R.R., Rolph, G.D., 2014. HYSPLIT (HYbrid Single-particle Lagrangian Integrated)

Durmusoglu, E., Taspinar, F., Karademir, A., 2010. Health risk assessment of BTEX emissions in the landfill environment. J. Hazard. Mater. 176, 870-877.

Fries, E., Sieg, K., Püttmann, W., Jaeschke, W., Winterhalter, R., Williams, J., Moortgat, G.K., 2008. Benzene, alkylated benzenes, chlorinated hydrocarbons and monoterpenes in snow/ice at Jungfraujoch (46.6 N, 8.0 E) during CLACE 4 and 5. Sci. Total Environ. 391, 269-277.

Fries, E., Starokozhev, E., Haunold, W., Jaeschke, W., Mitra, S.K., Borrmann, S., Schmidt, M.U., 2007. Laboratory studies on the uptake of aromatic hydrocarbons by ice crystals during vapor depositional crystal growth. Atmos. Environ. 41, 6156-6166.

Global Data Assimilation System, 2015. https://www.ready.noaa.gov/gdas1.php. Accessed: 27th Dec, 2015.

Goss, K.U., 1994. Predicting the enrichment of organic compounds in fog caused by adsorption on the water surface. Atmos. Environ. 28, 3513-3517.

Hall, M., Frank, E., Holmes, G., Pfahringer, B., Reutemann, P., Witten, I.H., 2009. The WEKA data mining software: an update. SIGKDD Explor. 11, 10-18.

Lin, C.C., Lin, C., Hsieh, L.T., Chen, C.Y., Wang, J.P., 2011. Vertical and diurnal characterization of volatile organic compounds in ambient air in urban areas. J. Air Waste. Manag. Assoc. 61, 714-720.

Lindinger, W., Hansel, A., Jordan, A., 1998. On-line monitoring of volatile organic compounds at pptv levels by means of Proton-Transfer-Reaction Mass Spectrometry (PTR-MS). Medical applications, food control and environmental research. Int. J. Mass Spectrom. Ion Process. 173, 191-241.

Lee, S.C., Chiu, M.Y., Ho, K.F., Zou, S.C. Wang, X., 2002. Volatile organic compounds (VOCs) in urban atmosphere of Hong Kong. Chemosphere 48, 375-382.

Matsumoto, K., Matsumoto, K., Mizuno, R., Igawa, M., 2010. Volatile organic compounds in ambient aerosols, Atmos. Res. 97, 124-128.

McNeill, V.F., Grannas, A.M., Abbatt, J.P., Ammann, M., Ariya, P., Bartels-Rausch, T., Domine, F., Donaldson, D.J., Guzman, M.I., Heger, D., Kahan, T.F., 2012. Organics in environmental ices: sources, chemistry, and impacts. Atmos. Chem. Phys. 12, 9653-9678.

Moreda-Piñeiro, J., Rodríguez, E.L., Pérez, C.M., Heras, G.B., Carou, I.T., Mahía, P.L., Lorenzo, S.M., Rodríguez, D.P., 2014. Influence of marine, terrestrial and anthropogenic sources on ionic and metallic composition of rainwater at a suburban site (Northwest Coast of Spain). Atmos. Environ. 88, 30-38.

Mullaugh, K.M., Hamilton, J.M., Avery, G.B., Felix, J.D., Mead, R.N., Willey, J.D., Kieber, R.J., 2015. Temporal and spatial variability of trace volatile organic compounds in rainwater. Chemosphere 134, 203-209.

Okochi, H., Kataniwa, M., Sugimoto, D., Igawa, M., 2005. Enhanced dissolution of volatile organic compounds into urban dew water collected in Yokohama, Japan. Atmos. Environ. 39, 6027-6036.

Okochi, H., Sugimoto, D., Igawa, M., 2004. The enhanced dissolution of some chlorinated hydrocarbons and monocyclic aromatic hydrocarbons in rainwater collected in Yokohama, Japan. Atmos. Environ. 38, 4403-4414.

O'Sullivan, D.W., Lee, M., Noone, B.C., Heikes, B.G., 1996. Henry's law constant determinations for hydrogen peroxide, methyl hydroperoxide, hydroxymethyl hydroperoxide, ethyl hydroperoxide, and peroxyacetic acid. J. Phys. Chem. 100, 3241–3247.

Perišić, M., Maletić, D., Stojić, S.S., Rajšić, S., Stojić, A., 2016, Forecasting hourly particulate matter concentrations based on the advanced multivariate methods. Int. J. Environ. Sci. Te. 1-8 .

Raja, S., Valsaraj, K.T., 2004. Adsorption and transport of gas-phase naphthalene on micron-size fog droplets in air. Environ. Sci. Technol. 38, 763-768.

Raja, S., Yaccone, F.S., Ravikrishna, R., Valsaraj, K.T., 2002. Thermodynamic parameters for the adsorption of aromatic hydrocarbon vapors at the gas−water interface. J. Chem. Eng. Data 47, 1213–1219.

Rao, P.S.P., Tiwari, S., Matwale, J.L., Pervez, S., Tunved, P., Safai, P.D., Srivastava, A.K., Bisht, D.S., Singh, S., Hopke, P.K., 2016. Sources of chemical species in rainwater during monsoon and nonmonsoonal periods over two megacities in India and dominant source region of secondary aerosols. Atmos. Environ. 146, 90-99.

Sander, R., 2015. Compilation of Henry's law constants (version 4.0) for water as solvent. Atmos. Chem. Phys. 15, 4399-4981.

Sapek, B., 2014. Calcium and magnesium in atmospheric precipitation, groundwater and the soil solution in long-term meadow experiments. J. Eleme. 19, 191-208.

Sato, E., Matsumoto, K., Okochi, H., Igawa, M., 2006. Scavenging effect of precipitation on volatile organic compounds in ambient atmosphere. Bull. Chem. Soc. Jpn. 79, 1231-1233.

Seinfeld, J.H. and Pandis, S.N., 2006. Atmospheric Chemistry and Physics: From Air Pollution to Climate Change, Second Ed., J. Wiley & Sons, New York.

Słomińska, M., Konieczka, P. and Namieśnik, J., 2014. The fate of BTEX compounds in ambient air. Crit. Rev. Env. Sci. Tec. 44, 455-472.

Šoštarić, A., Stojić, A., Stanišić, S.S., Gržetić, I., 2016. Quantification and mechanisms of BTEX distribution between aqueous and gaseous phase in a dynamic system. Chemosphere 144, 721-727.

Starokozhev, E., Fries, E., Cycura, A., Püttmann, W., 2009. Distribution of VOCs between air and snow at the Jungfraujoch high alpine research station, Switzerland, during CLACE 5 (winter 2006). Atmos. Chem. Phys. 9, 3197-3207.

Stojić, A., Stanišić, S.S., Reljin, I., Čabarkapa, M., Šoštarić, A., Perišić, M., Mijić, Z., 2016. Comprehensive analysis of PM10 in Belgrade urban area on the basis of long term measurements. Environ. Sci. Pollut. Res. 23, 10722-10732.

Stojić, A., Stanišić, S.S., Šoštarić, A., Ilić, L., Mijić Z., Rajšić, S., 2015a. Characterization of VOC sources in an urban area based on PTR-MS measurements and receptor modelling. Environ. Sci. Pollut. Res. 22, 13137-13152.

Stojić, A., Stojić, S.S., Mijić, Z., Ilić L., Tomašević, M., Todorović, M., Perišić, M. 2015b. Comprehensive analysis of VOC emission sources in Belgrade urban area. Urban and Built Environments, 55-88.

Stojić, A., Stojić, S.S., Mijić, Z., Šoštarić, A., Rajšić, S., 2015c. Spatio-temporal distribution of VOC emissions in urban area based on receptor modelling. Atmos. Environ. 106, 71-79.

Stojić, A., Maletić, D., Stojić, S.S., Mijić, Z., Šoštarić, A., 2015d. Forecasting of VOC emissions from traffic and industry using classification and regression multivariate methods. Sci. Total. Environ. 521, 19-26.

Stojić, A., Stanišić Stojić, S., 2017. The innovative concept of three-dimensional hybrid receptor modeling. Atmos. Environ. 164, 216–223.

Team, 2012. R: a Language and Environment for Statistical Computing. http://cran.case.edu/web/packages/dplR/vignettes/timeseries-dplR.pdf Accessed 4th December 2015.

Tiwari, S., Hopke, P.K., Thimmiah, D., Dumka, U.C., Srivastava, A.K., Bisht, D.S., Rao, P.S.P., Chate, D.M., Srivastava, M.K., Tripathi, S.N., 2016. Nature and sources of ionic species in precipitation across the Indo-Gangetic Plains, India. Aerosol Air Qual. Res. 16, 943-957.

USEPA, 2007. EPA Unmix 6.0 Fundamentals and User guide. USEPA Office of Research and Development.

Valsaraj, K.T., Thoma, G.J., Reible, D.D., Thibodeaux, L.J., 1993. On the enrichment of hydrophobic organic compounds in fog droplets. Atmos. Environ. 27, 203-210.

Vane, L.M., Giroux, E.L., 2000. Henry's law constants and micellar partitioning of volatile organic compounds in surfactant solutions. J. Chem. Eng. Data 45, 38-47.

Wang, Y.Q., 2014. MeteoInfo: GIS software for meteorological data visualization and analysis. Meteorol. Appl. 21, 360–368.

Warneke, C., De Gouw, J.A., Kuster, W.C., Goldan, P.D., Fall, R., 2003. Validation of atmospheric VOC measurements by proton-transfer-reaction mass spectrometry using a gas-chromatographic preseparation method. Environ. Sci. Technol. 37, 2494-2501.

WHO, 1997. Ethylbenzene Environmental Health Criteria 186. WHO, International Programme on Chemical Safety.

WHO, 1993. Benzene Environmental Health Criteria 150. WHO, International Programme on Chemical Safety.

WHO, 1986. Toluene Environmental Health Criteria 52. WHO, International Programme on Chemical Safety.

Highlights

- Potential of rainwater for BTEX scavenging from ambient air was examined
- BTEX concentrations in rain samples exceeded the theoretically predicted values
- BTEX retention could be associated with BTEX aerosol fraction
- Random forest and instance based algorithms provide reliable enrichment predictions
- Gas mixing ratios, rainwater characteristics and meteorology affect BTEX distribution